Cellular/Molecular

Unraveling Mechanisms Underlying Partial Agonism in 5-HT$_3$A Receptors

Jeremías Corradi and Cecilia Bouzat

Instituto de Investigaciones Bioquímicas de Bahía Blanca, Universidad Nacional del Sur-Consejo Nacional de Investigaciones Científicas y Técnicas, 8000 Bahía Blanca, Argentina

Partial agonists have emerged as attractive therapeutic molecules. 2-Me-5HT and tryptamine have been defined as partial agonists of 5-HT$_3$ receptors on the basis of macroscopic measurements. Because several mechanisms may limit maximal responses, we took advantage of the high-conductance form of the mouse serotonin type 3A (5-HT$_3$A) receptor to understand their molecular actions. Individual 5-HT-bound receptors activate in long episodes of high open probability, consisting of groups of openings in quick succession. The activation pattern is similar for 2-Me-5HT only at very low concentrations since profound channel blockade takes place within the activating concentration range. In contrast, activation episodes are significantly briefer in the presence of tryptamine. Generation of a full activation scheme reveals that the fully occupied receptor overcomes transitions to closed preopen states (primed states) before opening. Reduced priming explains the partial agonism of tryptamine. In contrast, 2-Me-5HT is not a genuine partial agonist since priming is not dramatically affected and its low apparent efficacy is mainly due to channel blockade. The analysis also shows that the first priming step is the rate-limiting step and partial agonists require an increased number of priming steps for activation. Molecular docking suggests that interactions are similar for 5-HT and 2-Me-5HT but slightly different for tryptamine. Our study contributes to understanding 5-HT$_3$A receptor activation, extends the novel concept of partial agonism within the Cys-loop family, reveals novel aspects of partial agonism, and unmasks molecular actions of classically defined partial agonists. Unraveling mechanisms underlying partial responses has implications in the design of therapeutic compounds.

Key words: **5-HT$_3$; kinetics; ligand-gated ion channel; patch clamp; serotonin; single channel**

Introduction

Cys-loop receptors are ligand-gated ion channels that include 5-HT$_3$, nicotinic (AChR), GABA, and glycine receptors. 5-HT$_3$ receptors are implicated in neurological disorders, are targets of antiemetic drugs, and are emerging as novel targets for a wide number of disorders, including schizophrenia, cognitive dysfunction, and pain (Walstab et al., 2010; Thompson, 2013).

Homomeric serotonin type 3A (5-HT$_3$A) receptors are functional. However, single-channel currents from these receptors cannot be detected due to their very low conductance (Maricq et al., 1991; Hussy et al., 1994; Mott et al., 2001). Mutations at the M3-M4 region lead to the high-conductance form of this receptor, which is a valid model for describing activation at the single-channel level (Kelley et al., 2003; Corradi et al., 2009).

Partial agonists have emerged as attractive therapeutic molecules because they can either act as agonists without producing overstimulation or decrease endogenous neurotransmitter activity without yielding the unfavorable effects that result from the use of antagonists. For ligand-gated ion channels, partial agonists have been simplistically defined as ligands that elicit submaximal currents at saturating concentrations. However, characterization of a genuine partial agonist is complex because other mechanisms, such as channel blockade or desensitization, limit maximal responses.

A novel interpretation for partial agonism has been recently proposed for AChRs and glycine receptors together with strong evidence supporting the theory that gating reaction in these receptors is not a simple isomerization from resting to open states (Colquhoun and Lape, 2012). Single-channel kinetic analysis from AChRs, glycine, and 5-HT$_3$A receptors revealed an intermediate high-affinity preopen state (flipped state) from which opening can occur (Lape et al., 2008; Corradi et al., 2009). Partial agonists are less effective because of their reduced ability to change the receptor conformation to this flipped state (Lape et al., 2008; Colquhoun and Lape, 2012). Thus, the differences between full and partial agonists lie largely in the rates from resting to flipped state, whereas rates for channel opening and closing are similar between them. An extension of the flip mechanism in which individual subunits flip independently, referred to as priming, has well described activation of mutant AChRs (Mukhtasimova et al., 2009) and mutant glycine receptors (Lape et al., 2012). Thus, single-channel kinetic analysis from receptors acti-

Received May 15, 2014; revised Oct. 16, 2014; accepted Oct. 20, 2014.

Author contributions: J.C. and C.B. designed research; J.C. and C.B. performed research; J.C. and C.B. analyzed data; J.C. and C.B. wrote the paper.

This work was supported by grants from the National Research Council of Argentina (Consejo Nacional de Investigaciones Científicas y Técnicas), Universidad Nacional del Sur, and Agencia Nacional de Promoción Científica y Tecnológica of Argentina.

The authors declare no competing financial interests.

Correspondence should be addressed to Dr. Cecilia Bouzat, Instituto de Investigaciones Bioquímicas, UNS-CONICET, Camino La Carrindanga Km 7, 8000 Bahía Blanca, Argentina. E-mail: inbouzat@criba.edu.ar.

DOI:10.1523/JNEUROSCI.1970-14.2014

 0270-6474/14/3316865-13$15.00/0

vated by partial agonists or in the presence of mutations has allowed the resolution of novel states that have added in-depth insight into the concept of partial agonism. In this scenario, we studied activation by two drugs thought to be 5-HT$_3$ partial agonists (Hussy et al., 1994; Bower et al., 2008). Our results demonstrate that 2-Me-5HT is an efficacious agonist but its maximal response is mainly limited by channel blockade. In contrast, tryptamine is a genuine partial agonist: its low efficacy is due to slow transitions from the fully liganded closed state to primed states. The kinetic analysis suggests that priming of the first subunit is the rate-limiting step for activation. Our study reveals the bases underlying partial agonism in a unexplored member of this receptor family, thus extending the next-generation activation model within the family, and provides novel information on the activation mechanism.

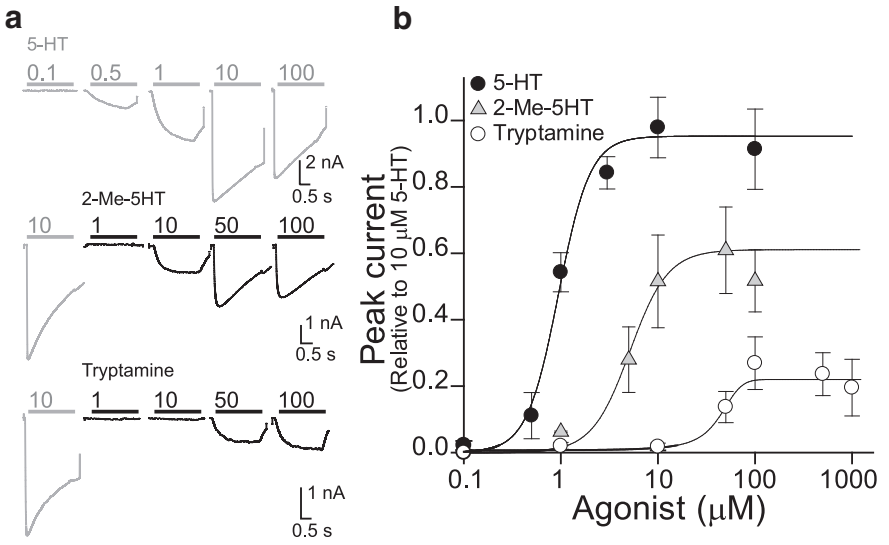

Figure 1. Macroscopic responses of 5-HT$_3$A receptors by different agonists. ***a***, Macroscopic currents recorded in the whole-cell configuration elicited by the three agonists at the indicated concentrations (in micromoles per liter). Membrane potential, − 50 mV. For 2-Me-5HT and tryptamine (black traces), currents were compared with those elicited by 10 μM 5-HT (gray trace) in the same cell. Solid lines represent the 2 s pulse for each ligand with the agonist concentration in micromoles. ***b***, Dose–response curves for 5-HT$_3$A receptors. All current amplitudes were normalized to those of 10 μM 5-HT-elicited currents and curves were fitted by the Hill equation. Data points are the means of >3 cells and bars indicate SD.

Materials and Methods

Expression of high-conductance 5-HT$_3$A receptors. The high-conductance forms of the 5-HT$_3$A receptor of mouse of either sex or α7–5HT$_3$A chimera were obtained by mutating three arginine residues responsible for the low conductance to glutamine, aspartic, and alanine as described previously (Kelley et al., 2003; Bouzat et al., 2004; Corradi et al., 2009, 2011). All experiments were performed with the high-conductance form of the receptors. BOSC 23 cells, which are modified HEK 293 cells (Pear et al., 1997), were transfected with the subunit cDNA and a plasmid encoding green fluorescent protein to allow identification of transfected cells.

Patch-clamp recordings. Single-channel currents were recorded in the cell-attached configuration at 20°C. The bath and pipette solutions contained 142 mM KCl, 5.4 mM NaCl, 0.2 mM $CaCl_2$, and 10 mM HEPES, pH 7.4, thus leading the membrane potential to be close to 0 mV. Agonists were added to the pipette solution. Single-channel currents were recorded and low-pass filtered to 10 kHz using an Axopatch 200 B patch-clamp amplifier (Molecular Devices), digitized at 5 μs intervals, analyzed manually, and detected by the half-amplitude threshold criterion using the TAC 4.0.10 program (Bruxton). Under these conditions, the inward conductance of the mouse high-conductance 5-HT$_3$A receptor is 67 pS (Corradi et al., 2009).

Open-time and closed-time histograms were plotted, using a logarithmic abscissa and a square-root ordinate (Sigworth and Sine, 1987), and fitted to the sum of exponential functions by maximum likelihood using the program TACFit 4.0.10 (Bruxton) with the dead time set at 30 μs. Bursts and clusters of channel openings were identified as a series of closely separated openings (>5) preceded and followed by closings longer than a critical duration. For defining bursts, the critical time was taken as the point of intersection of the second and the third component in the closed time histogram for bursts (τ_c^b). For defining clusters, the critical duration (τ_c^c) was taken as the point of intersection between the third closed component and the succeeding one, for 5-HT and tryptamine; or the fourth closed component and the succeeding one for 2-Me-5HT. Open probability within clusters (P_{open}) was determined by calculating the mean fraction of time that the channel is open within a cluster.

Macroscopic currents were recorded in the whole-cell configuration. The pipette solution contained 134 mM KCl, 5 mM EGTA, 1 mM $MgCl_2$, and 10 mM HEPES, pH 7.3. The extracellular solution (ECS) contained 150 mM NaCl, 0.5 mM $CaCl_2$, and 10 mM HEPES, pH 7.4. For dose–response curves, 2 s pulses of ECS containing different concentrations of agonist were applied. The solution exchange time was estimated by the open pipette and varied between 0.1 and 1 ms. Macroscopic currents were filtered at 5 kHz, digitized at 20 kHz, and analyzed using IgorPro software (WaveMetrics). Each current represents the average from three to five individual traces, which were obtained from the same cell and were aligned with each other at the point where they reached 50% of maximum. Currents were fitted by the following exponential function (Eq. 1): $I_{(t)} = I_0\ [\exp(-t/\tau_d] + I_\infty$, where I_0 and I_∞ are peak and the steady-state current values, respectively, and τ_d is the decay time constant. EC_{50} values from experimental or simulated data were obtained by fitting dose–response curves with the Hill equation as described previously (Corradi et al., 2009).

Single-channel kinetic analysis. For kinetic modeling, clusters were selected on the basis of their distribution of mean open duration and open probability (Corradi et al., 2009). Clusters showing open time and open probability values within two SDs of the mean of the major component were selected (~80% of the total). The resulting open and closed intervals, from single patches at different ligand concentrations, were analyzed according to a kinetic scheme using the QuB software (Qin et al., 1996; QuB suite, www.qub.buffalo.edu, State University of New York, Buffalo) as described previously (Corradi et al., 2009). The dead time was 25–30 μs. The model and the estimated rates were accepted if the resulting probability density functions correctly fitted the experimental open-duration and closed-duration histograms.

Estimation of rate constants from macroscopic currents was performed with QuB software by fitting the experimental currents on the basis of a given scheme. Agonist association and dissociation rate constants were estimated by using the macroscopic rate optimizer (MAC) algorithm included in the QuB package (Milescu et al., 2005). Simulation of single-channel and macroscopic currents were performed using QuB software based on the model proposed and using the rate constants for desensitization and recovery experimentally determined.

Statistical comparisons were performed with the Student's *t* test.

Molecular docking. A homology model for the extracellular region of the 5-HT$_3$A receptor was created based on the structure of the acetylcholine-binding protein engineered to recognize serotonin (Kesters et al., 2013; 5HTBP-AChBP; Protein Data Bank code: 2YMD). The amino acid sequence for the mouse 5HT$_3$A subunit (accession number: Q6JIJ7) was aligned with the sequence of the 5HTBP-AChBP using ClustalW and the homology modeling was performed using MODELLER 9v8

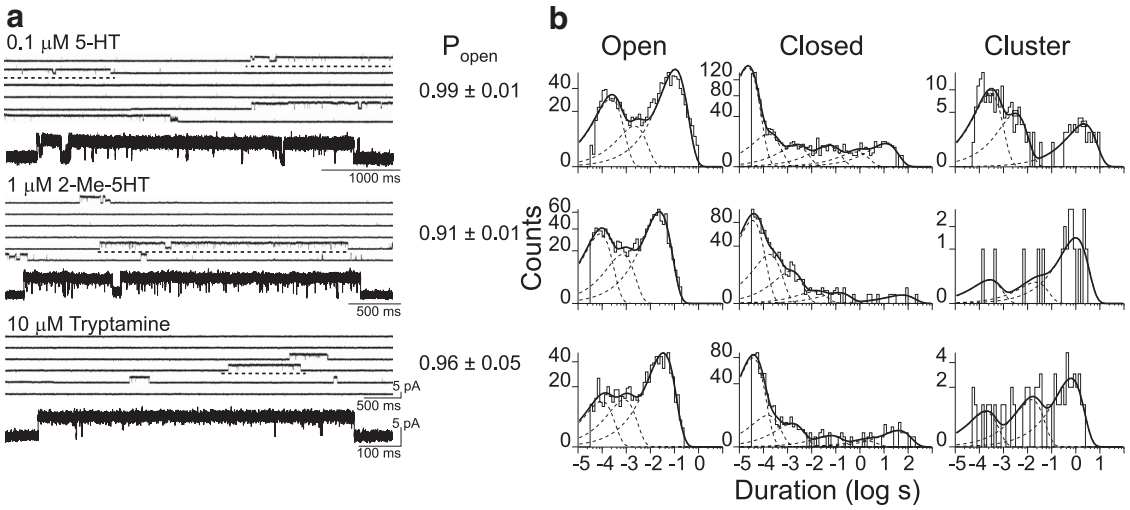

Figure 2. Single-channel currents evoked by low agonist concentrations. ***a***, Single-channel traces obtained in the cell-attached configuration at −70 mV membrane potential. For each agonist, the lowest concentration that evoked single-channel events is shown. Channel activity appears as long groups of openings separated by brief closings (bursts or clusters). The open probability for the activation episodes is indicated as the mean ± SD ($n > 3$ cells for each agonist). ***b***, Representative open-duration, closed-duration, and cluster-duration histograms obtained from the analysis of the whole recording.

Table 1. Open and closed durations of 5-HT$_3$A receptor channels in the presence of different ligands

Agonist	Concentration	O_B (area)	O_I (area)	O_L (area)	C_B (area)	C_I (area)	C_L (area)	C_{XL} (area)	*n*
5-HT									
	0.1 μM	0.19 ± 0.09 ms (0.50 ± 0.19)	1.0 ± 0.4 ms (0.13 ± 0.08)	106 ± 50 ms (0.37 ± 0.20)	0.05 ± 0.02 ms (0.54 ± 0.20)	0.37 ± 0.20 ms (0.19 ± 0.06)	2.6 ± 0.6 ms (0.08 ± 0.05)	—	5
	1 μM	0.14 ± 0.05 ms (0.49 ± 0.11)	2.4 ± 1.7 ms (0.13 ± 0.06)	113 ± 20 ms (0.38 ± 0.10)	0.04 ± 0.02 ms (0.54 ± 0.13)	0.30 ± 0.11 ms (0.26 ± 0.12)	2.7 ± 0.9 ms (0.11 ± 0.04)	—	8
	50 μM	0.18 ± 0.04 ms (0.13 ± 0.04)	3.6 ± 1.2 ms (0.29 ± 0.12)	11 ± 1 ms (0.58 ± 0.11)	0.02 ± 0.01 ms (0.80 ± 0.03)	0.13 ± 0.01 ms (0.10 ± 0.04)	3.3 ± 0.9 ms (0.04 ± 0.01)	—	3
	500 μM	0.40 ± 0.09 ms (0.12 ± 0.03)	—	1.5 ± 0.3 ms (0.77 ± 0.03)	0.03 ± 0.01 ms (0.79 ± 0.10)	0.14 ± 0.08 ms (0.14 ± 0.10)	1.8 ± 1.1 ms (0.03 ± 0.02)	—	3
2-Me-5HT									
	1 μM	0.10 ± 0.04 ms (0.28 ± 0.08)	0.84 ± 0.22 ms (0.14 ± 0.04)	20 ± 4 ms (0.59 ± 0.11)	0.05 ± 0.01 ms (0.70 ± 0.13)	0.20 ± 0.08 ms (0.17 ± 0.10)	2.2 ± 0.9 ms (0.08 ± 0.04)	16 ± 8 ms (0.02 ± 0.01)	5
	15 μM	0.08 ± 0.01 ms (0.27 ± 0.04)	—	4.2 ± 1.2 ms (0.73 ± 0.04)	0.05 ± 0.01 ms (0.80 ± 0.03)	0.26 ± 0.09 ms (0.08 ± 0.03)	1.6 ± 0.4 ms (0.09 ± 0.02)	16 ± 7 ms (0.02 ± 0.01)	5
	50 μM	0.06 ± 0.01 ms (0.25 ± 0.05)	—	1.3 ± 0.3 ms (0.75 ± 0.05)	0.05 ± 0.01 ms (0.88 ± 0.03)	0.36 ± 0.21 ms (0.08 ± 0.03)	1.5 ± 0.4 ms (0.03 ± 0.02)	26 ± 10 ms (0.02 ± 0.01)	3
	100 μM	0.07 ± 0.04 ms (0.40 ± 0.08)	—	0.93 ± 0.10 ms (0.60 ± 0.08)	0.04 ± 0.01 ms (0.82 ± 0.07)	0.26 ± 0.15 ms (0.09 ± 0.05)	0.96 ± 0.30 ms (0.06 ± 0.03)	9 ± 4 ms (0.02 ± 0.01)	4
Tryptamine									
	10 μM	0.15 ± 0.06 ms (0.36 ± 0.16)	1.3 ± 0.6 ms (0.14 ± 0.04)	31 ± 13 ms (0.51 ± 0.23)	0.04 ± 0.01 ms (0.65 ± 0.15)	0.22 ± 0.06 ms (0.25 ± 0.15)	2.4 ± 1.4 ms (0.07 ± 0.05)	—	9
	50 μM	0.16 ± 0.03 ms (0.24 ± 0.10)	2.2 ± 1.2 ms (0.15 ± 0.03)	24 ± 4 ms (0.48 ± 0.16)	0.03 ± 0.01 ms (0.78 ± 0.04)	0.17 ± 0.08 ms (0.17 ± 0.04)	1.5 ± 0.9 ms (0.03 ± 0.01)	—	5
	100 μM	0.15 ± 0.04 ms (0.37 ± 0.21)	1.5 ± 0.6 ms (0.15 ± 0.05)	8 ± 2 ms (0.51 ± 0.15)	0.06 ± 0.04 ms (0.70 ± 0.18)	0.31 ± 0.11 ms (0.22 ± 0.15)	2.0 ± 0.9 ms (0.04 ± 0.03)	—	5
	500 μM	0.20 ± 0.06 ms (0.19 ± 0.10)	—	1.2 ± 0.2 ms (0.86 ± 0.13)	0.04 ± 0.01 ms (0.83 ± 0.15)	0.16 ± 0.04 ms (0.15 ± 0.12)	1.0 ± 0.3 ms (0.05 ± 0.02)	—	4

Single-channel recordings of the high-conductance form of 5-HT$_3$A receptor in the presence of different concentrations of each agonist.

Clusters were identified as successive openings separated by closings briefer than a critical duration (see Materials and Methods). Open-time histograms, constructed with openings of the whole recording, were fitted by three components (O_B, O_I, and O_L) at low agonist concentrations and by two components at higher concentrations due to open channel blockade. Closed-time histograms from the whole recording show 5–6 closed components but the table shows the three briefest components (C_B, C_I, and C_L) that correspond to closings within clusters. C_{XL} corresponds to the new closed component detected in the presence of 2-Me-5HT.

Results are shown as the mean duration ± SD and *n* corresponds to the number of patches for each condition.

(Sali and Blundell, 1993). Ten models were generated. Of these, the one with the lowest energy and the smallest percentage of amino acids in the disallowed region of the Ramachandran plot was selected for docking studies. The protonated form of each agonist was docked into the binding site region between subunits E and A using AUTODOCK 4.2 (Goodsell et al., 1996). A hundred genetic algorithm runs were performed for each docking study.

Results

2-Me-5HT and tryptamine elicit submaximal macroscopic responses

To evaluate the overall behavior of two serotonin receptor ligands, 2-Me-5HT and tryptamine, we recorded macroscopic currents in the whole-cell configuration from cells expressing

5-HT$_3$A receptors. Application of the full agonist, 5-HT, elicits currents whose decays are well fitted by a single exponential component (Eq. 1; Fig. 1*a*). Expressing the relative peak current as a function of 5-HT concentration results in EC_{50} values of 0.94 ± 0.09 μM and Hill coefficient (nH) of 2.7 ± 0.7 (Fig. 1*b*). Macroscopic currents elicited by 1–100 μM 2-Me-5HT or 1–1000 μM tryptamine show slower onset compared with those elicited by 5-HT. The rise time, measured from the $t_{20-80\%}$ at saturating concentrations, is 18 ± 8 ms for 10 μM 5-HT, 60 ± 20 ms for 100 μM 2-Me-5HT, and 50 ± 7 ms for 100 μM tryptamine.

When compared with 5-HT, dose–response curves for 2-Me-5HT and tryptamine show higher EC_{50} values [5.2 ± 0.6 μM (nH, 2.2 ± 0.7) and 40 ± 3 μM (nH, 2.0 ± 0.3), respectively] and smaller maximal responses (0.60 ± 0.03 and 0.22 ± 0.01, respectively), in good agreement with data previously reported (Hussy et al., 1994; van Hooft and Vijverberg, 1996; Hu et al., 2003; Bower et al., 2008). Together, these results confirm that 2-Me-5HT and tryptamine are apparent partial agonists of the high-conductance 5-HT$_3$A receptor.

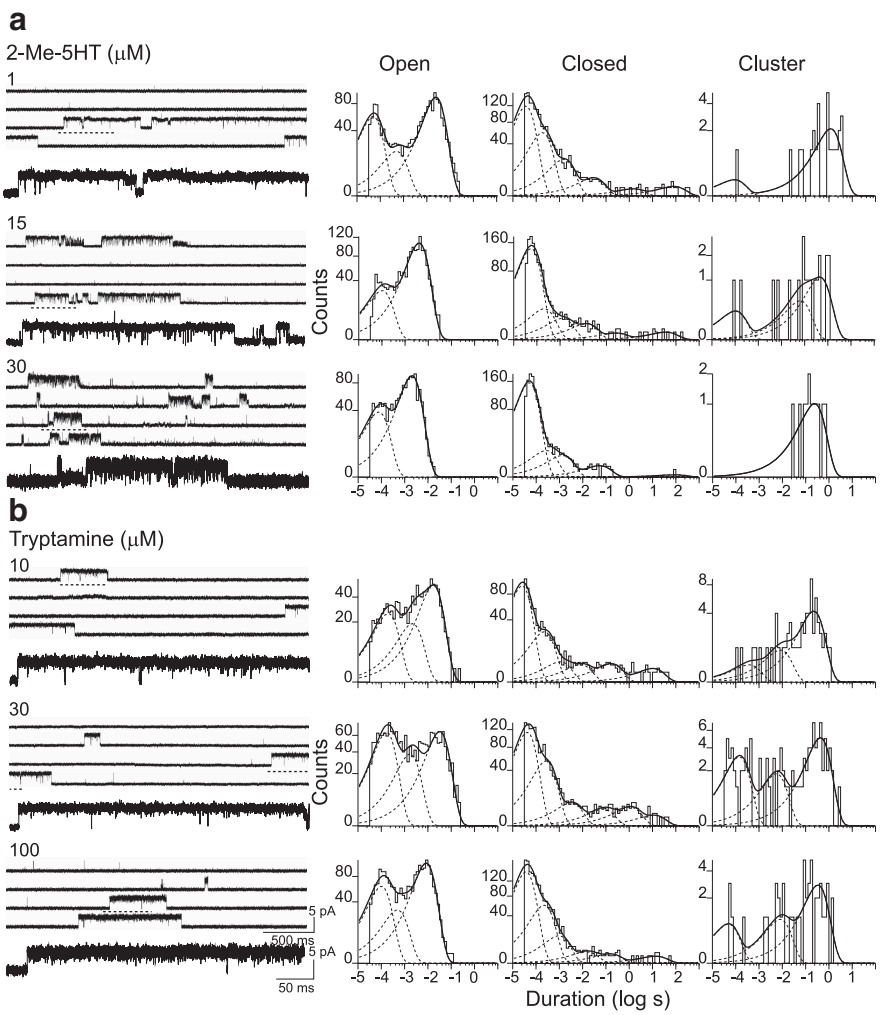

Figure 3. ***a***, ***b***, Single-channel activity in the presence of 2-Me-5HT (***a***) or tryptamine (***b***). Left, Representative single-channel recordings from cell-attached patches at different agonist concentrations. Membrane potential, − 70 mV. The upper part of each single-channel recording shows continuous sweeps for each agonist concentration, and the selected portion (dashed lines) is shown below in a higher time resolution. Right, Representative open-duration, closed-duration, and cluster-duration histograms obtained from the analysis of the whole recording for each agonist concentration.

Single-channel activity in the presence of 2-Me-5HT and tryptamine

To determine the molecular mechanism underlying partial responses, we explored activation at the single-channel level.

At all 5-HT concentrations (≥0.1 μM) single-channel activity from cell-attached patches is readily detected (Corradi et al., 2009, 2011). Opening events of ~4.7 pA (−70 mV) appear in quick succession grouped in bursts of high open probability, which coalesce into long clusters of ~2 s (Corradi et al., 2009). Each cluster corresponds to an activation episode of a single receptor molecule. Open-time histograms from the analysis of the entire recording show three components whose durations are ~200 μs, ~2.5 ms, and ~110 ms (Fig. 2*b*; Table 1). The three classes of openings occur within clusters since open-time histograms constructed with only selected clusters also show three components. The mean duration of the longest open component clearly decreases at concentrations >3 μM due to 5-HT open-channel blockade (Corradi et al., 2009). At 500 μM of 5-HT, open-time histograms are fitted by only two components as a consequence of significant channel block (Table 1).

At all 5-HT concentrations, closed-time histograms are fitted by 5–6 components, where the three briefest correspond to closings within clusters (Fig. 2*b*; Table 1). The open probability (0.99) is constant at all agonist concentrations below the blocking ones (Fig. 2*a*). Thus, the frequency of clusters but not their properties differs among different 5-HT concentrations (below the ones producing open-channel blockade; Corradi et al., 2009).

In the presence of 2-Me-5HT or tryptamine, bursts of openings in quick succession separated by brief closings are detected (Fig. 2*a*). The lowest agonist concentrations that allow reliable opening detection are 10-fold and 100-fold higher for 2-Me-5HT (1 μM) and tryptamine (10 μM), respectively, than for 5-HT (0.1 μM).

At 1 μM 2-Me-5HT, open-time histograms are fitted by three components whose durations are ~100 μs, ~1 ms, and ~20 ms (Table 1). The duration of the slowest component shows a clear decrease as a function of drug concentration (Fig. 3*a*). At concentrations >5 μM, open-time histograms are fitted by only two components as a consequence of channel block (Fig. 3*a*; Table 1). Closed-time histograms are fitted by 5–6 components at all concentrations. The four briefest components correspond to closings within clusters and their mean durations are constant at all 2-Me-5HT concentrations. An increase in the area of the briefest closed component with the increase in 2-Me-5HT concentration is observed (Table 1). The decrease of the open time and increase in the proportion of brief closings suggest open-channel block (Neher and Steinbach, 1978).

At all 2-Me-5HT concentrations, channel activity appears as long clusters of high P_{open} composed of ~2–3 bursts, similar to 5-HT clusters (Fig. 3*a*). Cluster duration and P_{open} decrease as a

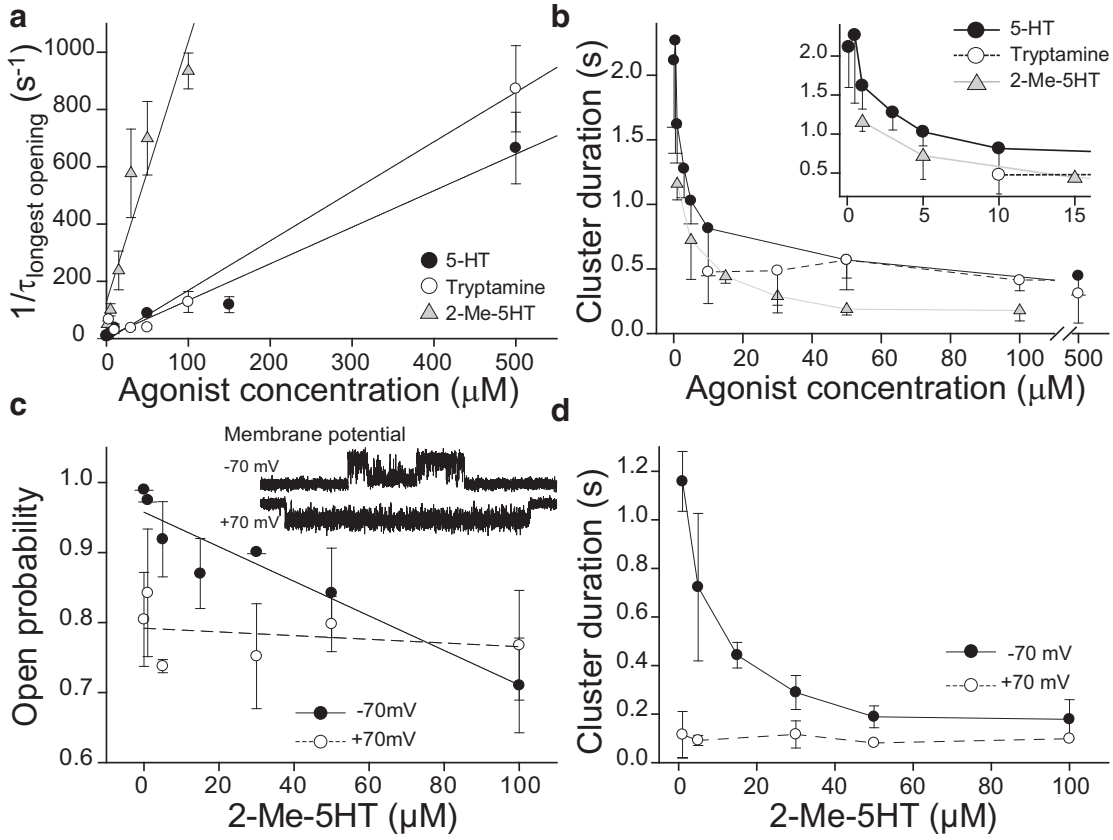

Figure 4. Channel blockade of 5-HT$_3$A receptors. ***a***, Relationship between the inverse of the longest-duration open component and agonist concentration. Data were fitted by the linear equation $1/\tau_{open} = \alpha + k_{+B}[Ag]$, where k_{+B} is the forward blocking rate constant and α is the apparent channel closing rate. ***b***, Cluster duration as a function of agonist concentration. For clarity, error bars are shown in only one direction. The inset shows the curves at higher resolution for concentrations <20 μM. ***c***, Open probability for clusters at different 2-Me-5HT concentrations at −70 mV and +70 mV of membrane potential. For all plots, each point represents the mean ± SD of >3 recordings. The inset shows representative clusters obtained at the two different membrane potentials. ***d***, Cluster duration as a function of 2-Me-5HT concentration at +70 mV and −70 mV.

function of agonist concentration for 5-HT and, more profoundly, for 2-Me-5HT (Figs. 3*a*, 4*b*).

Thus, it is possible to identify two types of inhibitory effects associated with the increase in agonist concentration, one mainly evidenced by the decrease in the duration of opening events and the other by the decrease in cluster duration.

For tryptamine, single-channel recordings show that despite its low efficacy (~22% in whole-cell recordings) activation also occurs in bursts of high P_{open} (>0.9; Fig. 3*b*). However, bursts do not coalescence into long clusters as in the presence of 5-HT or 2-Me-5HT; they instead appear isolated, thus leading to significantly shorter activation episodes (Fig. 3*b*). Open time histograms of channels recorded at tryptamine concentrations from 10 to 50 μM show three components of ~150 μs, ~2 ms, and ~30 ms (Table 1; Fig. 3*b*). At >50 μM tryptamine, a clear reduction in the duration of the slowest open component is observed (Table 1). Closed-time histograms show 5–6 components, where the three briefest are constant at all agonist concentrations with durations similar to those observed in the presence of 5-HT or 2-Me-5HT (Table 1).

At 10 μM tryptamine, the mean burst (τ^b_{crit}, ~0.4–1.5 ms) and cluster duration (τ^c_{crit}, ~3–15 ms) are 370 ± 190 and 380 ± 190 ms, respectively, thus confirming that the main form of activation elicited by tryptamine is in isolated bursts and not in long clusters. Increasing 10-fold the critical time for cluster selection does not change the burst duration, confirming the result. Thus, for tryptamine, each cluster is composed of only one burst. Interestingly, clusters are composed of the three classes of openings and closings and show high P_{open} (~0.95 at concentrations <500 μM). Mean durations of closed periods within clusters are constant at all tryptamine concentrations, and are similar to those observed for 5-HT and 2-Me-5HT. There is an increase in the area of the briefest closed component with the increase of tryptamine concentration (Table 1). The reduction in the duration of the slowest open component and the increase in the area of the briefest closed component suggest open-channel blockade, though this occurs at a significantly higher concentration range than for 2-Me-5HT.

Together, the main differences at the single-channel level between the partial agonists and 5-HT are (1) the profound channel blockade that takes place within the activating concentration range for 2-Me-5HT and (2) the presence of isolated bursts instead of long clusters for tryptamine.

Open-channel blockade

Because blockade seems to be significant, especially for 2-Me-5HT, we analyzed this mechanism in detail. We first evaluated fast-channel blockade that leads to the reduction of open duration, which we call B_1 block. On the basis of a simple open-channel block mechanism, the slope of the linear relationship between the inverse of the mean duration of the slowest open component and agonist concentration allows estimation of the forward blocking constant (k_{+B1}). The estimated k_{+B1} value is similar for 5-HT ($1.3 \times 10^6\ M^{-1}\ s^{-1}$, $r^2 = 0.98$) and tryptamine

($1.7 \times 10^6\ M^{-1}\ s^{-1}$, $r^2 = 0.98$), whereas it is one order of magnitude higher for 2-Me-5HT ($1.6 \times 10^7\ M^{-1}\ s^{-1}$, $r^2 = 0.90$), indicating its higher open-channel blocker potency (Fig. 4*a*).

Because the area of the briefest closed component increases with drug concentration in parallel with the decrease of the duration of the slowest open component, we associated this closed component with the fast-blocking process. In this scenario, the inverse of the mean duration of the closed component provides an estimation of the unblocking rate constant (k_{-B1}, ~20,000 s^{-1}). Thus, the estimated blocking constants, K_{B1} (k_{-B1}/k_{+B1}), are 17, 1, and 15 mM for 5-HT, 2-Me-5HT, and tryptamine, respectively. This result demonstrates that 2-Me-5HT, as an open-channel blocker, is ~15-fold more potent than 5-HT and tryptamine. Single-channel amplitudes remain constant at the range of agonist concentrations assayed. Only at the highest tested concentration of each agonist is there a slight (8–10%) and statistically significant reduction of channel amplitude (4.2 ± 0.1 pA at 500 μM 5-HT, $p < 0.05$; 3.4 ± 0.7 pA at 100 μM 2-Me-5HT, $p < 0.05$; and 4.0 ± 0.3 pA at 500 μM tryptamine, $p < 0.05$), indicating that the majority of channel blockages are resolved at the concentrations used for the kinetic analysis.

In addition to the reduction in open duration, cluster duration also decreases as a function of concentration for 5-HT and 2-Me-5HT (Fig. 4*b*). At the concentration corresponding to the EC_{50} value for each agonist, cluster duration is not affected for 5-HT and tryptamine, whereas it is reduced by 40% for 2-Me-5HT (Fig. 4*b*). Because the reduction in the mean open time is due to open-channel blockade, an increase in cluster duration as a function of blocker concentration would be expected (Neher and Steinbach, 1978). Therefore, the decrease of cluster duration could be explained by two possible mechanisms: (1) a mechanism in which the blocked receptor closes or desensitizes (see Fig. 6, Scheme 1), as reported previously for the AChR (Murrell et al., 1991; Dilger et al., 1997); and (2) a mechanism that involves an additional, long-lived, blocked state (B_2) occurring from the open state through a concentration-dependent transition (see Fig. 6, Scheme 2).

To further explore the inhibitory actions of 2-Me-5HT, we recorded channels at +70 mV (membrane potential) at a range of drug concentration (Fig. 4*c*,*d*). At this positive membrane potential, open probability and cluster duration show no significant changes with the increase of drug concentration, in contrast to the observations at −70 mV. Thus, the inhibitory effect of 2-Me-5HT is voltage dependent as expected for channel blockers (Bertrand et al., 1990). Moreover, macroscopic current recordings show that the maximal peak current elicited by 2-Me-5HT is 40% lower than that elicited by 5-HT at −50 mV membrane potential ($p < 0.05$, $n = 7$; Fig. 1), whereas it is similar to that of 5-HT at +50 mV ($p > 0.1$, $n = 7$), thus confirming the voltage dependence of 2-Me-5HT inhibition.

Finally, to confirm that 2-Me-5HT and tryptamine act as blockers of the 5-HT$_3$ pore, we evaluated their effect on the α7–5HT$_3$A chimeric receptor, which contains the extracellular domain of α7 AChR and the transmembrane and intracellular region of 5-HT$_3$ (Bouzat et al., 2004; Rayes et al., 2005; Corradi et al., 2009). Single-channel openings activated by 500 μM ACh show reduced mean open duration as a function of concentration of the serotoninergic ligands present in the pipette solution. The

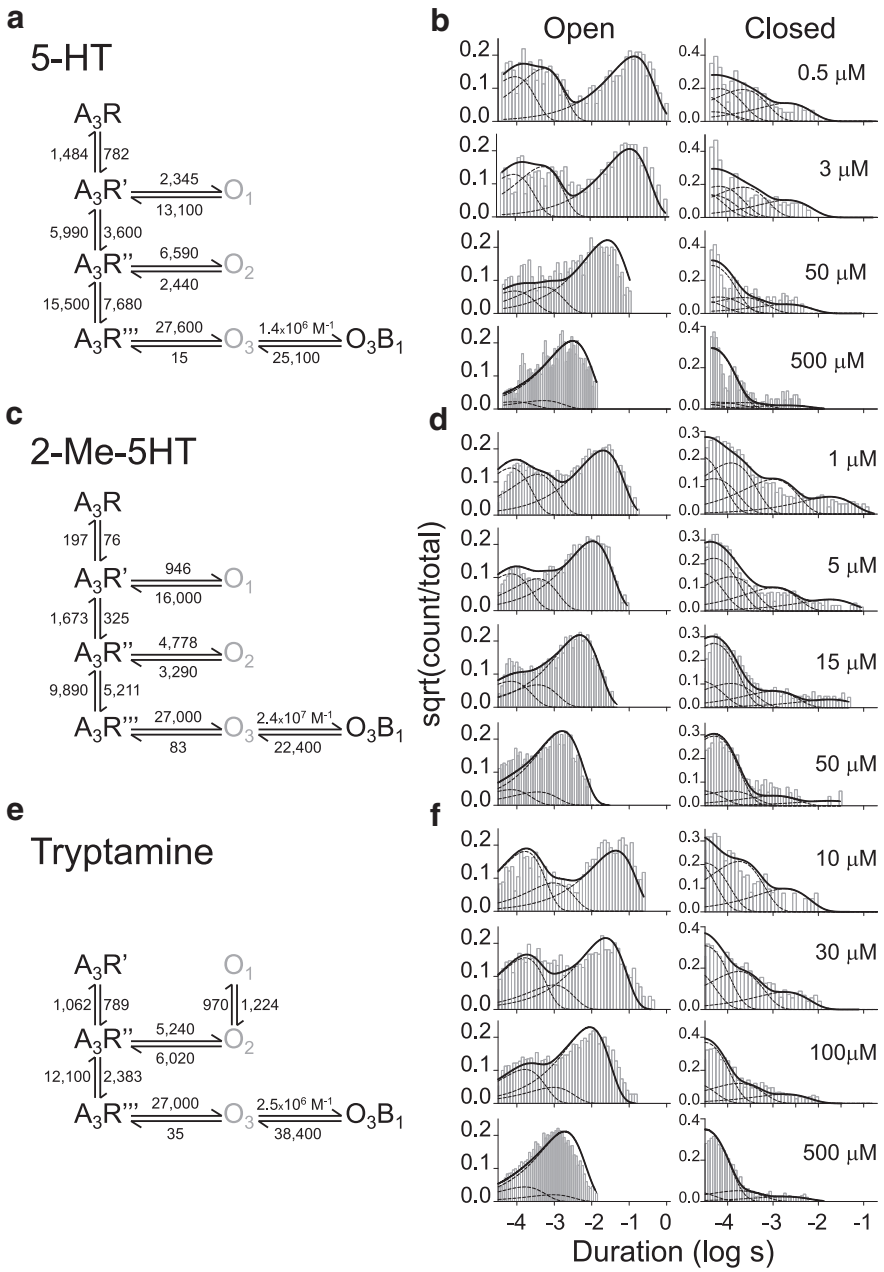

Figure 5. Kinetic analysis for 5-HT$_3$A receptors activated by the different agonists. Kinetic analysis was restricted to clusters, for 5-HT and 2-Me-5HT, or to bursts, for tryptamine. For each transition, the mean value of the rate is shown as s^{-1}. On the right of each scheme (***a***, ***c***, ***e***), the experimental open-duration and closed-duration histograms at different agonist concentrations with the theoretical curves superimposed are shown (***b***, ***d***, ***f***).

mean duration of the slowest open component, which is 9.0 ± 2.4 ms ($n = 7$) in the control, is reduced to 4.0 ± 1.3 and 1.20 ± 0.05 ms at 5 and 30 μM 2-Me-5HT, and to 5.3 ± 1.0 and 0.3 ± 0.1 ms at 50 and 500 μM tryptamine, respectively. On the basis of a linear blocking scheme, this reduction yields estimated values for k_{+B1} of 2.5×10^7 M^{-1} s^{-1} ($r^2 = 0.93$) for 2-Me-5HT and 4.9×10^6 M^{-1} s^{-1} ($r^2 = 0.99$) for tryptamine, which is in close agreement with those estimated for 5-HT$_3$A receptors.

Together, the analysis shows that for 2-Me-5HT, the activation pattern, which consists of long clusters of high P_{open}, is similar to that of 5-HT only at the lowest concentration that allows channel detection or at positive membrane potentials since the concentration range for channel blockade overlaps with that for activation. For tryptamine, higher agonist concentrations are required for channel detection, indicating that it is the less potent of the tested agonists. Blockade is not significantly different to that produced by 5-HT and the main difference in the activation profile resides in the presence of isolated bursts that do not coalescence into long clusters as with 5-HT.

Kinetic modeling for partial agonist activation

To identify a plausible mechanism that could explain why these two agonists partially activate 5-HT$_3$A receptors, we performed kinetic analyses using data from macroscopic and single-channel recordings.

Primed mechanism

We have previously generated a model for 5-HT$_3$A activation that includes a flip or preopen state from the receptor with three occupied binding sites, which is sufficient for maximal activation (Corradi et al., 2009). In this scheme, the three open states are connected to two intraburst and one interburst intracluster closed states. However, this scheme cannot describe 2-Me-5HT activation since single-channel recordings show four closed components within clusters instead of three. On the other hand, primed models have been applied to partial agonists acting on AChR and glycine receptors (Mukhtasimova et al., 2009; Lape et al., 2012). In this scenario, we inferred that the primed model would be better to describe 5-HT$_3$A activation by partial agonists.

As a first approach we fitted macroscopic currents, obtained at different agonist concentrations, using the MAC algorithm from the QuB Suite (see Materials and Methods) to obtain information about binding and priming steps. Supported by the lack of concentration dependence, we assumed that activation mostly occurs when the receptor has reached the most favorable occupation state (A_3R), and therefore we did not consider openings from double-liganded and monoliganded states (Corradi et al., 2009). For this macroscopic analysis, we considered a simplified model with three agonist binding steps, which are required for maximal responses (Solt et al., 2007; Corradi et al., 2009) and a single opening. To account for the high open probability within bursts for all agonists, fast open–closed transitions are required. However, such transitions cannot explain the low efficacy observed in macroscopic currents. For this reason, it is required to include a preopen step that limits the efficacy of channel activation. The main difference in channel activation elicited by full and partial agonists resides therefore in the first priming step (Fig. 5, from A_3R to A_3R'). The results show that the affinity of the agonist for the resting state is not greatly reduced. In particular, the estimated k_2/k_1 value is similar for tryptamine and 5-HT (Table 2), indicating that the reduced affinity by itself cannot explain the reduction in EC_{50} values and maximal responses.

Table 2. Kinetic parameters for 5-HT$_3$A receptor activated by different agonists

		5-HT	2-Me-5HT	Tryptamine
δ_3'	[s^{-1}]	782 ± 67	76 ± 7	2 ± 1
γ_3'	[s^{-1}]	1,484 ± 233	197 ± 20	1,130 ± 680
δ_3''	[s^{-1}]	3,600 ± 680	325 ± 27	789 ± 60
γ_3''	[s^{-1}]	5,990 ± 1,435	1,673 ± 150	1,062 ± 114
ϵ_3''	[s^{-1}]	—	—	1,224 ± 182
ξ_3''	[s^{-1}]	—	—	970 ± 154
δ_3'''	[s^{-1}]	7,680 ± 1,120	5,211 ± 480	2,383 ± 162
γ_3'''	[s^{-1}]	15,500 ± 1,350	9,890 ± 1,025	12,100 ± 1,050
β_3'	[s^{-1}]	2,345 ± 370	946 ± 58	—
α_3'	[s^{-1}]	13,100 ± 1,200	16,000 ± 804	—
β_3''	[s^{-1}]	6,590 ± 560	4,778 ± 290	5,595 ± 267
α_3''	[s^{-1}]	2,440 ± 213	3,290 ± 217	5,736 ± 266
β_3'''	[s^{-1}]	27,600 ± 2,350	27,000*	27,000*
α_3'''	[s^{-1}]	15 ± 1	83 ± 4	35 ± 2
F		0.53 ± 0.09	0.40 ± 0.05	0.002 ± 0.001
F'		0.60 ± 0.18	0.20 ± 0.02	0.74 ± 0.10
F''		0.50 ± 0.08	0.53 ± 0.07	0.20 ± 0.02
θ_3'		0.18 ± 0.03	0.06 ± 0.01	—
θ_3''		2.7 ± 0.3	1.3 ± 0.1	0.98 ± 0.06
θ_3'''		1,840 ± 200	325 ± 16	770 ± 44
k_1	[M^{-1}s^{-1}] × 10^6	15 ± 9	1.0 ± 0.6	60 ± 30
k_2	[s^{-1}]	150 ± 90	37 ± 17	620 ± 250
k_3	[s^{-1}]	0.27*	0.27*	0.27*
R	[s^{-1}]	0.01*	0.01*	0.01*
k_{+B1}	[M^{-1}s^{-1}] × 10^6	1.4 ± 0.1	24 ± 1	2.5 ± 0.1
k_{-B1}	[s^{-1}]	25,100 ± 920	22,400 ± 516	38,400 ± 1,322
d_+	[s^{-1}]	1.2*	1.2*	1.2*
d_-	[s^{-1}]	0.01*	0.01*	0.01*
c_+		400 ± 200	400*	400*
c_-	[s^{-1}]	<1	<1*	<1*
k_{+B2}	[M^{-1}s^{-1}] × 10^3	118 ± 75	50*	1.8*
k_{-B2}	[s^{-1}]	<1	<1*	<1*

Kinetic parameters corresponding to the activation scheme shown in Figure 7.

For tryptamine, the rates for the first priming (δ_3') and unpriming (γ_3') were determined from macroscopic current analysis. For 5-HT and 2-Me-5HT, the rates shown in the table were determined from cluster analysis. Similar values were determined from macroscopic currents (124 ± 33 s^{-1} and 690 ± 130 s^{-1} for 5-HT, and 102 ± 60 s^{-1} and 477 ± 285 s^{-1} for 2-Me-5HT, for δ_3' and γ_3', respectively). For 5-HT, c_+, c_-, k_{+B2}, and k_{-B2} were estimated from the fit of macroscopic currents. For 2-Me-5HT and tryptamine, k_{+B2} was estimated from the decrease of cluster duration as a function of agonist concentration. k_3, d_+, and d_- for 5-HT were constrained to values reported previously (Corradi et al., 2009). For 2-Me-5HT and tryptamine β_3''', k_3, d_+, d_-, c_+, c_-, and k_{-B2} were constrained to values obtained for 5-HT to allow a better fit and good representation of the simulated data. Rates are expressed as mean ± SE for at least three different patches. The equilibrium constants are $F = \delta/\gamma$ for priming and $\theta = \beta/\alpha$ for gating.

*Constrained rates.

We next fitted clusters obtained from single-channel recordings in the presence of 5-HT or 2-Me-5HT to the primed scheme using the Maximum Interval Likelihood algorithm from the QuB Suite (see Materials and Methods). Because all agonists produce fast open-channel blockade, we connected a block state to the longest-duration open state in each scheme (Fig. 5), and fitted these schemes to a set of single-channel recordings obtained at different agonist concentrations. For both agonists, open-time and closed-time histograms are well described by the theoretical curves (Fig. 5*b*,*d*). Thus, the models describe well open-time and closed-time histograms, and show similar rates for open–closed transitions within clusters (Fig. 5*a*–*d*; Table 2). The main difference between both agonists is observed in the transition from the resting state at the maximal occupation needed for activation (A_3R) to the first primed state (A_3R') (Table 2), which corresponds to closings between bursts and within clusters. As shown by the estimated equilibrium constants (F'), this transition is slightly less efficient for 2-Me-5HT than for 5-HT ($F'_{2\text{-Me-5HT}}$, ~0.40; $F'_{5\text{-HT}}$, ~0.50, where $F' = \delta'/\gamma'$; Table 2). It is important to remark that the rates for the first priming transition obtained

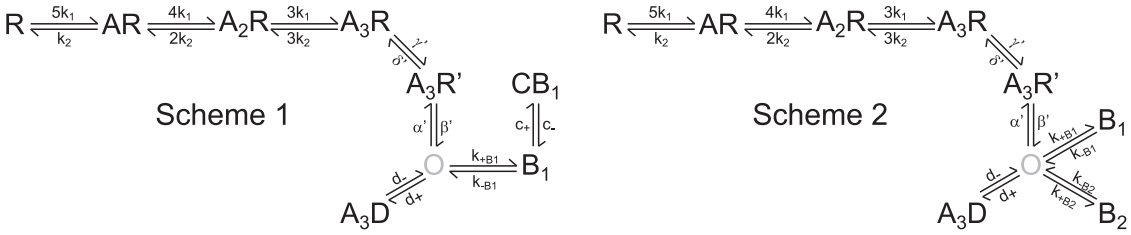

Figure 6. Kinetic schemes that explain the reduction in cluster duration as a function of agonist concentration. The simplified models have three binding steps (R to A_3R), one primed (A_3R'), one open (O), one desensitized (A_3D), and a fast-block state (B_1). Scheme 1 includes a closed or desensitized state (CB_1) connected to B_1. Scheme 2 includes a second block state (B_2). The duration of both states, CB_1 and B_2, are longer than the critical time used for cluster selection.

from the single-channel data are very similar to those obtained from the macroscopic current analysis (Table 2).

In the presence of tryptamine, activation occurs in isolated bursts, i.e., each cluster is composed of a single burst. Therefore, we first fitted single-channel data to the same model as that for 5-HT but lacking the interburst intracluster closed state (A_3R-to-A_3R' transition). This reduced model could not describe open time distributions because the rates for the first primed-open transition (A_3R' to O_1), and in consequence O_1, could not be solved. Because our single-channel analysis revealed that the three classes of openings occur within a burst, we next tested whether open components could be well described by using an alternative model in which the first primed-open transition (A_3R' to O_1) was excluded but the O_1 and O_2 states were connected, allowing the representation of the three open states (Fig. 5*e*). On the basis of this model, the theoretical curves superimposed well on the experimental histograms (Fig. 5*f*).

A remarkable aspect of the results of our kinetic analysis is that the first priming step is the one that limits the efficacy of partial agonists; in other words, once the receptor overcomes this transition, the second and third priming steps are faster and more similar to those for 5-HT (Table 2, compare values for *F*', *F*", *F*"').

Another remarkable finding revealed by the analysis is that the gating equilibrium constant for each open state increases as a function of the priming step, and three primed subunits are required for the maximal open-channel stability for all agonists. The gating equilibrium constants for all open states slightly differ among agonists (Table 2, compare θ_3', θ_3", and θ_3"'). The gating equilibrium constant θ_3"' is only ~2.4-fold lower for tryptamine than 5-HT. However, the equilibrium constant for the first priming step (*F*') is ~250-fold lower for tryptamine with respect of that of 5-HT.

Thus, the kinetic analysis from single-channel recordings provided information about priming, open, closing, and fast-blocking steps, and that from macroscopic currents about binding and priming steps. To obtain a complete activation scheme, we still needed to include the steps underlying the decrease in cluster duration. We therefore modeled the two possible mechanisms leading to this decrease (Fig. 6, Schemes 1 and 2) because there is no way of identifying from the experimental data which of the two takes place.

Scheme 1 incorporates a nonconducting state (CB_1) arising from closing or desensitization of the blocked state (B_1), as reported previously for the AChR (Murrell et al., 1991; Dilger et al., 1997). Although the B_1-to-CB_1 transition is not dependent on agonist concentration, CB_1 will increase with concentration due to the concentration dependence of the preceding step, which is also voltage dependent. Scheme 2 includes an additional, long-lived, blocked state (B_2) connected to the open state through a concentration-dependent transition.

We have previously determined that the decrease of cluster duration as a function of 5-HT follows the decrease in the decay time constant of macroscopic currents obtained from rapidly perfused outside-out patches (Corradi et al., 2009). Therefore, for 5-HT, c_+ and c_- (Fig. 6, Scheme 1) and k_{+B2} and k_{-B2} (Fig. 6, Scheme 2) were estimated by fitting the decay of macroscopic currents obtained from outside-out patches at a range of concentration using MAC (QuB software; Table 2). However, currents elicited by tryptamine and 2-Me-5HT are too small to be measured from outside-out patches and whole-cell currents do not allow reliable estimates of the decay time constants. Therefore, for these agonists, c_+, c_-, and k_{-B2} were constrained to those determined for 5-HT (Table 2), and k_{+B2} was estimated from the decrease of cluster duration as a function of agonist concentration (Fig. 4*b*; Table 2).

Combining the rate constants resulting from macroscopic and single-channel kinetic analysis leads to the full scheme shown in Figure 7 with the corresponding rate constants in Table 2.

Based on this kinetic model, both single-channel and macroscopic simulations reproduce well the experimental results (Fig. 7*b*,*c*). Macroscopic current simulations show the changes in efficacy for channel activation by 2-Me-5HT and tryptamine with respect to 5-HT (Fig. 7*b*). Single-channel simulations also resemble the experimental data for the three agonists and show the reduction in open time and cluster duration due to fast and slow blockade (Fig. 7*c*). No differences of the simulated channels and currents were observed between the two possible mechanisms underlying cluster duration decrease. The fact that it is not possible to ascertain which of these two mechanisms leads to slow blockade does not affect our conclusion that 2-Me-5HT is not a genuine partial agonist. In fact, at the lowest tested concentration, at which block is not significant, the simulated data well reproduce the experimental data for 2-Me-5HT (Fig. 7).

The final scheme revealed the basis underlying partial responses. 2-Me-5HT is partial mainly because of its potent action as a channel blocker in addition to its slightly reduced priming. In contrast, tryptamine behaves as a genuine low-efficacy agonist and shows significantly reduced priming, which results in the lack of long activation episodes.

Molecular docking of partial agonists

To visualize how the agonists interact with the binding site, we performed molecular docking studies using a homology model for the extracellular domain of 5-HT$_3$ and the protonated forms of each agonist (Fig. 8). The docking results show 5-HT in two main possible orientations with similar binding energy but different frequency (Fig. 8, Models 1 and 2). These orientations are similar to those previously reported (Price et al., 2008; Thompson et al., 2010), but slightly different to those in the template 5HTBP-AChBP structure, which corresponds to AChBP con-

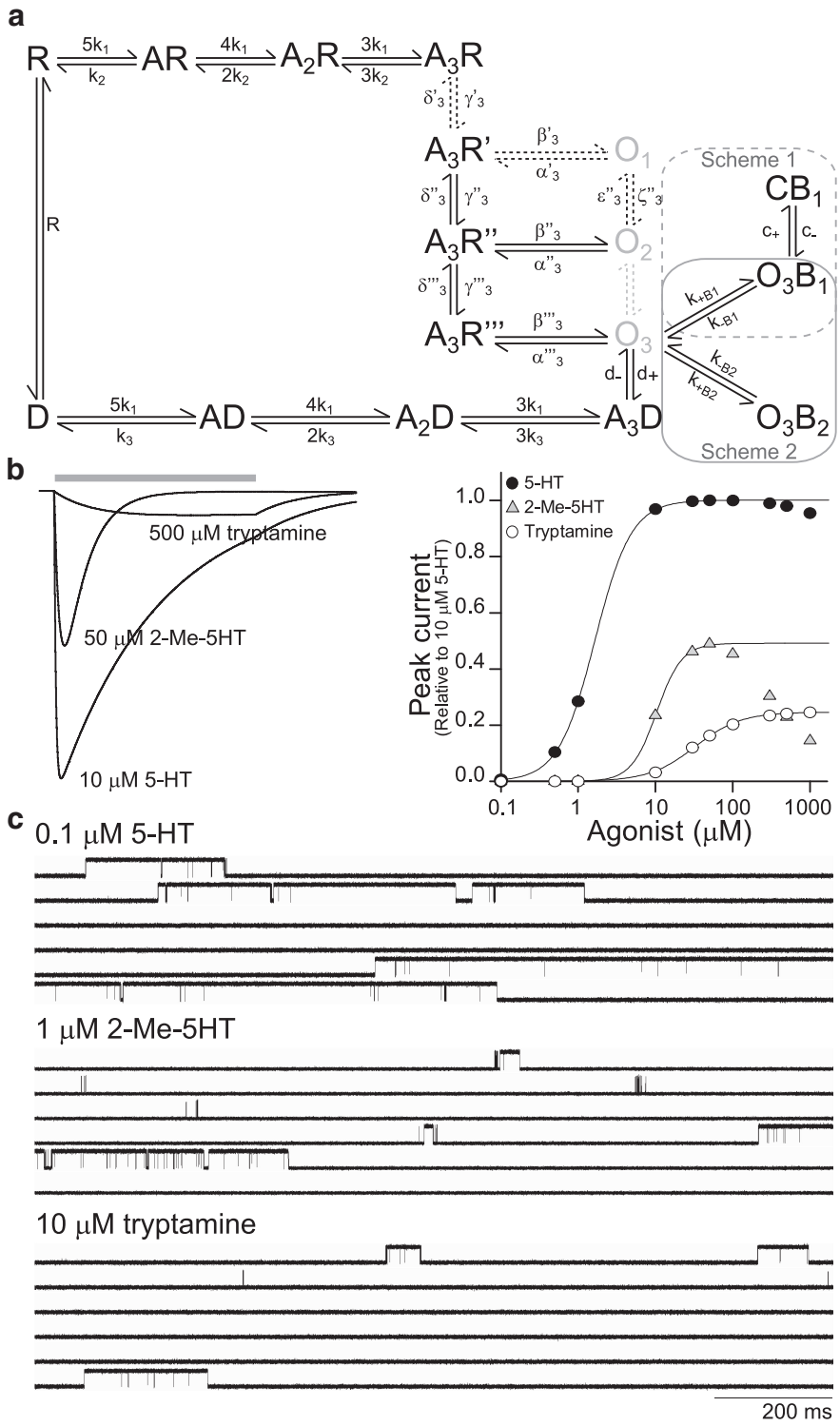

Figure 7. Single-channel and macroscopic current simulations. ***a***, Full activation scheme that explains 5-HT$_3$A receptor activation by the three agonists. Dashed black arrows represent the kinetic transitions that are mainly affected by the efficacy of the agonist. The dashed gray arrow between O_2 and O_3 is shown to suggest the possible transition. The complete scheme includes the two possible blocking mechanisms leading to cluster reduction (dashed line box for Scheme 1 and solid line box for Scheme 2). Kinetic constants are shown in Table 2. ***b***, Left, Macroscopic currents simulated on the basis of the complete scheme shown in ***a***. For the simulations, we considered 1000 receptors and a single-channel amplitude of 4.6 pA. Right, Simulated dose–response curves. Each point corresponds to the peak of the simulated current relative to the peak of the current simulated at 10 μM 5-HT. Simulated data were fitted to the Hill equation. ***c***, Simulated single-channel currents for each agonist at the shown concentration. Simulations correspond to the complete scheme, including Scheme 2, as the mechanism of slow block. No differences in the simulated currents were observed when Scheme 1 was used instead.

taining key 5-HT$_3$ residues at the binding site (Kesters et al., 2013).

Model 1 (Fig. 8) is the most frequently observed conformation (>50%), where the amino group of 5-HT has the potential to make cation-π interactions with W183, F226, and Y234, H-bonds with E129 of the principal face, and cation-π interaction with W90 of the complementary face. This model also shows the indol nitrogen of 5-HT making an H-bond with Y234 in loop C (principal face). Mutagenesis experiments have demonstrated that these residues are important for channel function (Price and Lummis, 2004; Suryanarayanan et al., 2005; Price et al., 2008). In Model 2 (Fig. 8), the amino group of 5-HT makes cation-π interaction only with W183, and the aromatic ring of 5-HT is involved in π–π interaction with W90. The main difference with Model 1 is that the hydroxyl group of 5-HT is orientated toward E129 making an H-bond, an interaction that has been suggested as critical for binding and gating (Sullivan et al., 2006; Price et al., 2008; Miles et al., 2012). Both models show potential interactions with residues from loop E (Y141, Y143, and/or Y153), which could be important for activation (Beene et al., 2004; Hazai et al., 2009; Kesters et al., 2013). Docking results for 2-Me-5HT are similar to those of 5-HT (Fig. 8), suggesting that both agonists have the same capability to interact with the binding site.

For tryptamine, docking analysis shows the two main conformations represented by Models 1 and 2 with similar interactions to those of 5-HT and 2-Me-5HT (Fig. 8). However, because tryptamine lacks the hydroxyl group, H-bonds with Y141, Y143, Y153, and Y234 (Model 1) or with E129 (Model 2) are missing, suggesting that they could be important for determining ligand efficacy, as previously described (Price et al., 2008).

Discussion

It has been recently shown that partial agonism in AChR and glycine receptors is not a property of the open–closed transition as has been supposed for the last 50 years. Instead, it arises in the earlier conformational change from the resting state to an intermediate preopen conformational state (Lape et al., 2008; Mukhtasimova et al., 2009). Global fitting of schemes to single-channel data for AChR and glycine receptors has allowed the identification of closed intermediate states that may represent activation intermediates between the agonist-bound resting state and the opening of the channel.

The conformational changes leading to these intermediate states may be concerted (flip model; Burzomato et al., 2004; Corradi et al., 2009; Sivilotti, 2010) or not, which involves individual "priming" of each binding site (Mukhtasimova et al., 2009; Lape et al., 2012). These observations have revised the classical model of activation of these receptors from a scheme comprising agonist binding and channel gating steps, to a new one comprising agonist binding, priming or flipping, and channel gating (Lape et al., 2008, 2012; Corradi et al., 2009; Mukhtasimova et al., 2009; Krashia et al., 2011). The intermediate preopen states determine agonist efficacy and they therefore contribute to synaptic responses.

We here explore molecular bases underlying partial agonism in a not-yet-characterized Cys-loop receptor, the 5-HT$_3$A receptor. Our results reveal that, as in related receptors, reduced priming explains the partial agonism of tryptamine at 5-HT$_3$A receptors. They also show that 2-Me-5HT, which has been considered a typical low-efficacy partial agonist, is a potent channel blocker. This distinction has significant implications for rational drug design since changes in membrane potential may have great variations in the efficacy of drugs whose partial responses are due to channel blockade. Thus, this finding enhances the importance of single-channel kinetic studies for all ligand-gated ion channels.

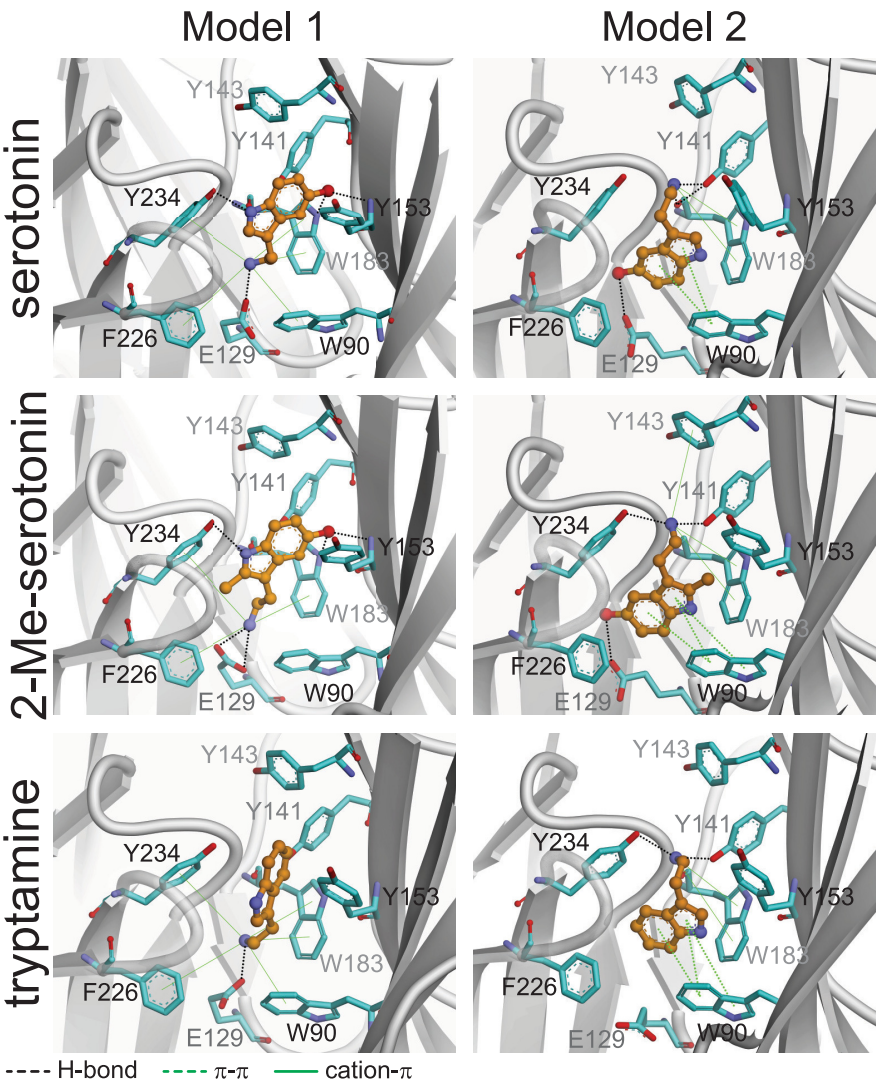

Figure 8. Molecular docking of ligands into the 5-HT$_3$A binding site. The model was obtained by homology modeling of the structure of the acetylcholine binding protein engineered to recognize serotonin (Kesters et al., 2013; 5HTBP-AChBP; Protein Data Bank code: 2YMD). The figure shows the two possible orientations for each agonist. The agonist orientation and interactions with residues in the binding pocket are similar for 5-HT and 2-Me-5HT.

Single-channel characterization of 5-HT$_3$A receptors has lagged behind because of its low conductance and its complex kinetics. To overcome the low conductance, we used the high-conductance form of this receptor (Kelley et al., 2003), whose activation properties are similar to those of the wild type (Corradi et al., 2009). A unique feature of 5-HT-elicited single-channel activity is that openings appear in clusters even at the lowest concentration that allows detectable openings. Clusters, which are composed of bursts of closely spaced openings, show, independently of agonist concentration, high P_{open} and three open states and three or four closed states (Corradi et al., 2009, 2011). At concentrations below the blocking ones, the activation pattern by 2-Me-5HT is almost indistinguishable to that elicited by 5-HT. In contrast, tryptamine elicits isolated bursts of high P_{open} that are not grouped into the typical 1–2 s clusters. However, the high P_{open} of bursts cannot explain the dramatic changes observed at the macroscopic level when compared with 5-HT responses, represented by ~20% of maximal response, 40-fold increased EC_{50} value, and threefold increased rise time. Results from our single-channel kinetic analysis revealed explanations for this apparent controversy.

We previously generated a model for 5-HT$_3$A receptors activated by 5-HT that describes binding, gating, and desensitization, and includes a concerted conformational change of the triple-liganded receptor to an activatable state while the channel is still shut (Corradi et al., 2009), similar to the flip model first reported for glycine receptors (Lape et al., 2008). We here applied kinetic analysis for two classical partial agonists and found that the flipped model, which contains only one preopen state, cannot well describe the experimental data. We therefore applied the primed model, as required before for mutant glycine receptors (Lape et al., 2012). Kinetic analysis from single-channel recordings, which provides information about priming, open, and closing transitions, was combined with that from macroscopic current recordings to obtain a complete activation model that also includes agonist binding and desensitization (Fig. 7; Table 2). The general model shows that after binding three molecules of agonist, the receptor overcomes the first priming transition to a closed preopen state (Fig. 7*a*, A$_3$R') from where it can either open or prime to A$_3$R" and A$_3$R"' states (Fig. 7*a*). From each primed state, the receptor is able to open; and the gating equilibrium constant increases with priming. Interestingly, tryptamine cannot lead to channel opening from the first primed state (Fig. 5*e*), in close agreement with its low efficacy. This observation suggests

that partial agonists require an increased number of primed subunits to allow activation.

The main conclusions from our kinetic analysis are as follows: (1) the low efficacy of tryptamine, and to a lesser extent of 2-Me-5HT, is due to reduced priming; (2) the first priming step seems to be the rate-limiting step for gating, and priming seems to be highly cooperative among subunits (in other words, once a subunit has primed, priming is faster for the rest); (3) the first priming transition is the one that mostly differs among agonists, whereas opening and closing transitions are similar among agonists; (4) the gating equilibrium constant increases with priming (i.e., it is higher in receptors with three primed subunits than with only one; Table 2, compare θ_3', θ_3", and θ_3"'); and (5) the open-channel duration increases with priming, as shown before for AChR (Mukhtasimova et al., 2009). For 5-HT_3A receptors, the maximal open duration is achieved after three primed steps for all agonists.

At low agonist concentration, at which block is minimized, 2-Me-5HT has slightly reduced efficacy compared with 5-HT due to a threefold decreased affinity and a 0.8-fold reduced priming equilibrium constant for the first priming transition (F'). This agrees with the fact that the activation pattern observed at a very low 2-Me-5HT concentration is almost identical to that of 5-HT. Thus, block seems to be the main cause leading to reduced responses of 5-HT_3A receptors by 2-Me-5HT. 2-Me-5HT differs only in a methyl group from 5-HT, which may therefore be an important substituent regarding open-channel blockade. In addition to the reduction of mean open time as a function of agonist concentration, there is a significant reduction in cluster duration. This observation indicates a deviation of the classical open-channel block mechanism (Gurney and Rang, 1984; Dilger and Liu, 1992; Bouzat and Barrantes, 1993, 1996; Arias et al., 2006; Corradi et al., 2011), which could be due to closing or desensitization of the blocked receptor, or to additional slow blockade (Gurney and Rang, 1984; Amador and Dani, 1991; Murrell et al., 1991; Dilger and Liu, 1992; Dilger et al., 1997). Since reduction in open time and cluster duration depends directly or indirectly on agonist concentration and voltage, we cannot identify which of the two mechanisms takes place. Moreover, currents and single channels simulated on the basis of activation schemes including either mechanism reproduce well the experimental data. Therefore, the uncertainty about which of them is involved in slow block does not affect our final conclusion. Although 5-HT also induces slow blockade (Corradi et al., 2009), it is the potency and not the blocking mechanism that makes 2-Me-5HT behave as a partial agonist because it shows overlapped concentration ranges for blocking and activation.

In contrast, tryptamine does not produce significantly increased block with respect to 5-HT, and it behaves as a genuine partial agonist. Its reduced efficacy is well explained by a ~250-fold reduced priming equilibrium constant. Once priming has been achieved, the opening–closing transition is remarkably similar to that of full agonists. Reduced priming explains why tryptamine elicits submaximal responses but at the same time generates a stable open state interrupted by brief closings.

Our docking study shows that the type and frequency of interactions of 5-HT and 2-Me-5HT at the binding site are similar. The lack of the hydroxyl group of tryptamine affects its capability to make H-bond interactions with residues at the binding site. Particularly E129 (detected in Model 2) has been shown to be important for ligand binding and channel activation in 5-HT_3A receptors (Price et al., 2008) and the equivalent residue, Y93, has also been shown to be important in AChR function (Aylwin and White, 1994).

Overall, our study contributes to the understanding of the mechanism of activation of 5-HT_3A receptors, extends the novel concept of partial agonism to other Cys-loop receptors, reveals novel aspects of partial agonism, and provides new information for understanding the mechanism of activation in the Cys-loop receptor family. Deciphering the molecular bases underlying submaximal responses has implications in the future for the design of partial agonists for therapeutic use (Manning et al., 2011; Revel et al., 2012).

References

Amador M, Dani JA (1991) MK-801 inhibition of nicotinic acetylcholine receptor channels. Synapse 7:207–215. CrossRef Medline

Arias HR, Bhumireddy P, Bouzat C (2006) Molecular mechanisms and binding site locations for noncompetitive antagonists of nicotinic acetylcholine receptors. Int J Biochem Cell Biol 38:1254–1276. CrossRef Medline

Aylwin ML, White MM (1994) Ligand-receptor interactions in the nicotinic acetylcholine receptor probed using multiple substitutions at conserved tyrosines on the alpha subunit. FEBS Lett 349:99–103. CrossRef Medline

Beene DL, Price KL, Lester HA, Dougherty DA, Lummis SC (2004) Tyrosine residues that control binding and gating in the 5-hydroxytryptamine3 receptor revealed by unnatural amino acid mutagenesis. J Neurosci 24:9097–9104. CrossRef Medline

Bertrand D, Ballivet M, Rungger D (1990) Activation and blocking of neuronal nicotinic acetylcholine receptor reconstituted in Xenopus oocytes. Proc Natl Acad Sci U S A 87:1993–1997. CrossRef Medline

Bouzat C, Barrantes FJ (1993) Hydrocortisone and 11-desoxycortisone modify acetylcholine receptor channel gating. Neuroreport 4:143–146. CrossRef Medline

Bouzat C, Barrantes FJ (1996) Modulation of muscle nicotinic acetylcholine receptors by the glucocorticoid hydrocortisone. Possible allosteric mechanism of channel blockade. J Biol Chem 271:25835–25841. CrossRef Medline

Bouzat C, Gumilar F, Spitzmaul G, Wang HL, Rayes D, Hansen SB, Taylor P, Sine SM (2004) Coupling of agonist binding to channel gating in an ACh-binding protein linked to an ion channel. Nature 430:896–900. CrossRef Medline

Bower KS, Price KL, Sturdee LE, Dayrell M, Dougherty DA, Lummis SC (2008) 5-Fluorotryptamine is a partial agonist at 5-HT_3 receptors, and reveals that size and electronegativity at the 5 position of tryptamine are critical for efficient receptor function. Eur J Pharmacol 580:291–297. CrossRef Medline

Burzomato V, Beato M, Groot-Kormelink PJ, Colquhoun D, Sivilotti LG (2004) Single-channel behavior of heteromeric $\alpha 1\beta$ glycine receptors: an attempt to detect a conformational change before the channel opens. J Neurosci 24:10924–10940. CrossRef Medline

Colquhoun D, Lape R (2012) Perspectives on: conformational coupling in ion channels: allosteric coupling in ligand-gated ion channels. J Gen Physiol 140:599–612. CrossRef Medline

Corradi J, Gumilar F, Bouzat C (2009) Single-channel kinetic analysis for activation and desensitization of homomeric 5-HT_3A receptors. Biophys J 97:1335–1345. CrossRef Medline

Corradi J, Andersen N, Bouzat C (2011) A novel mechanism of modulation of 5-HT_3A receptors by hydrocortisone. Biophys J 100:42–51. CrossRef Medline

Dilger JP, Liu Y (1992) Desensitization of acetylcholine receptors in BC3H-1 cells. Pflugers Arch 420:479–485. CrossRef Medline

Dilger JP, Boguslavsky R, Barann M, Katz T, Vidal AM (1997) Mechanisms of barbiturate inhibition of acetylcholine receptor channels. J Gen Physiol 109:401–414. CrossRef Medline

Goodsell DS, Morris GM, Olson AJ (1996) Automated docking of flexible ligands: applications of AutoDock. J Mol Recognit 9:1–5. CrossRef Medline

Gurney AM, Rang HP (1984) The channel-blocking action of methonium compounds on rat submandibular ganglion cells. Br J Pharmacol 82:623–642. CrossRef Medline

Hazai E, Joshi P, Skoviak EC, Suryanarayanan A, Schulte MK, Bikadi Z (2009) A comprehensive study on the 5-hydroxytryptamine(3A) recep-

tor binding of agonists serotonin and m-chlorophenylbiguanidine. Bioorg Med Chem 17:5796–5805. CrossRef Medline

Hu XQ, Zhang L, Stewart RR, Weight FF (2003) Arginine 222 in the pre-transmembrane domain 1 of 5-HT$_3$A receptors links agonist binding to channel gating. J Biol Chem 278:46583–46589. CrossRef Medline

Hussy N, Lukas W, Jones KA (1994) Functional properties of a cloned 5-hydroxytryptamine ionotropic receptor subunit: comparison with native mouse receptors. J Physiol 481:311–323.

Kelley SP, Dunlop JI, Kirkness EF, Lambert JJ, Peters JA (2003) A cytoplasmic region determines single-channel conductance in 5-HT$_3$ receptors. Nature 424:321–324. CrossRef Medline

Kesters D, Thompson AJ, Brams M, van Elk R, Spurny R, Geitmann M, Villalgordo JM, Guskov A, Danielson UH, Lummis SC, Smit AB, Ulens C (2013) Structural basis of ligand recognition in 5-HT$_3$ receptors. EMBO Rep 14:49–56. CrossRef Medline

Krashia P, Lape R, Lodesani F, Colquhoun D, Sivilotti LG (2011) The long activations of alpha2 glycine channels can be described by a mechanism with reaction intermediates ("flip"). J Gen Physiol 137:197–216. CrossRef Medline

Lape R, Colquhoun D, Sivilotti LG (2008) On the nature of partial agonism in the nicotinic receptor superfamily. Nature 454:722–727. CrossRef Medline

Lape R, Plested AJ, Moroni M, Colquhoun D, Sivilotti LG (2012) The α1K276E startle disease mutation reveals multiple intermediate states in the gating of glycine receptors. J Neurosci 32:1336–1352. CrossRef Medline

Manning DD, Cioffi CL, Usyatinsky A, Fitzpatrick K, Masih L, Guo C, Zhang Z, Choo SH, Sikkander MI, Ryan KN, Naginskaya J, Hassler C, Dobritsa S, Wierschke JD, Earley WG, Butler AS, Brady CA, Barnes NM, Cohen ML, Guzzo PR (2011) Novel serotonin type 3 receptor partial agonists for the potential treatment of irritable bowel syndrome. Bioorg Med Chem Lett 21:58–61. CrossRef Medline

Maricq AV, Peterson AS, Brake AJ, Myers RM, Julius D (1991) Primary structure and functional expression of the 5HT$_3$ receptor, a serotonin-gated ion channel. Science 254:432–437. CrossRef Medline

Miles TF, Bower KS, Lester HA, Dougherty DA (2012) A coupled array of noncovalent interactions impacts the function of the 5-HT$_3$A serotonin receptor in an agonist-specific way. ACS Chem Neurosci 3:753–760. CrossRef Medline

Milescu LS, Akk G, Sachs F (2005) Maximum likelihood estimation of ion channel kinetics from macroscopic currents. Biophys J 88:2494–2515. CrossRef Medline

Mott DD, Erreger K, Banke TG, Traynelis SF (2001) Open probability of homomeric murine 5-HT3A serotonin receptors depends on subunit occupancy. J Physiol 535:427–443. CrossRef Medline

Mukhtasimova N, Lee WY, Wang HL, Sine SM (2009) Detection and trapping of intermediate states priming nicotinic receptor channel opening. Nature 459:451–454. CrossRef Medline

Murrell RD, Braun MS, Haydon DA (1991) Actions of n-alcohols on nicotinic acetylcholine receptor channels in cultured rat myotubes. J Physiol 437:431–448. Medline

Neher E, Steinbach JH (1978) Local anaesthetics transiently block currents through single acetylcholine-receptor channels. J Physiol 277:153–176. Medline

Pear WS, Scott ML, Nolan GP (1997) Generation of high-titer, helper-free retroviruses by transient transfection. Methods Mol Med 7:41–57. Medline

Price KL, Lummis SC (2004) The role of tyrosine residues in the extracellular domain of the 5-hydroxytryptamine3 receptor. J Biol Chem 279:23294–23301. CrossRef Medline

Price KL, Bower KS, Thompson AJ, Lester HA, Dougherty DA, Lummis SC (2008) A hydrogen bond in loop A is critical for the binding and function of the 5-HT3 receptor. Biochemistry 47:6370–6377. CrossRef Medline

Qin F, Auerbach A, Sachs F (1996) Estimating single-channel kinetic parameters from idealized patch-clamp data containing missed events. Biophys J 70:264–280. CrossRef Medline

Rayes D, Spitzmaul G, Sine SM, Bouzat C (2005) Single-channel kinetic analysis of chimeric alpha7–5HT3A receptors. Mol Pharmacol 68:1475–1483. CrossRef Medline

Revel FG, Moreau JL, Gainetdinov RR, Ferragud A, Velázquez-Sánchez C, Sotnikova TD, Morairty SR, Harmeier A, Groebke Zbinden K, Norcross RD, Bradaia A, Kilduff TS, Biemans B, Pouzet B, Caron MG, Canales JJ, Wallace TL, Wettstein JG, Hoener MC (2012) Trace amine-associated receptor 1 partial agonism reveals novel paradigm for neuropsychiatric therapeutics. Biol Psychiatry 72:934–942. CrossRef Medline

Sali A, Blundell TL (1993) Comparative protein modelling by satisfaction of spatial restraints. J Mol Biol 234:779–815. CrossRef Medline

Sigworth FJ, Sine SM (1987) Data transformations for improved display and fitting of single-channel dwell time histograms. Biophys J 52:1047–1054. CrossRef Medline

Sivilotti LG (2010) What single-channel analysis tells us of the activation mechanism of ligand-gated channels: the case of the glycine receptor. J Physiol 588:45–58. CrossRef Medline

Solt K, Ruesch D, Forman SA, Davies PA, Raines DE (2007) Differential effects of serotonin and dopamine on human 5-HT3A receptor kinetics: interpretation within an allosteric kinetic model. J Neurosci 27:13151–13160. CrossRef Medline

Sullivan NL, Thompson AJ, Price KL, Lummis SC (2006) Defining the roles of Asn-128, Glu-129 and Phe-130 in loop A of the 5-HT3 receptor. Mol Membr Biol 23:442–451. CrossRef Medline

Suryanarayanan A, Joshi PR, Bikádi Z, Mani M, Kulkarni TR, Gaines C, Schulte MK (2005) The loop C region of the murine 5-HT3A receptor contributes to the differential actions of 5-hydroxytryptamine and m-chlorophenylbiguanide. Biochemistry 44:9140–9149. CrossRef Medline

Thompson AJ (2013) Recent developments in 5-HT3 receptor pharmacology. Trends Pharmacol Sci 34:100–109. CrossRef Medline

Thompson AJ, Lester HA, Lummis SC (2010) The structural basis of function in Cys-loop receptors. Q Rev Biophys 43:449–499. CrossRef Medline

van Hooft JA, Vijverberg HP (1996) Selection of distinct conformational states of the 5-HT3 receptor by full and partial agonists. Br J Pharmacol 117:839–846. CrossRef Medline

Walstab J, Rappold G, Niesler B (2010) 5-HT(3) receptors: role in disease and target of drugs. Pharmacol Ther 128:146–169. CrossRef Medline